CONF-8906184--3

Received by OSTI

AUG 0 4 1989

SAND--89-1208C

DE89 015887

HYDROGEN AND DEUTERIUM PROFILING IN POLYMERS USING LIGHT AND HEAVY ION ELASTIC RECOIL DETECTION*

Peter F. Green and Barney L. Doyle

Sandia National Laboratories, Albuquerque, N.M. 87185-5800

DISCLAIMER

This report was prepared as an account of work sponsored by an agency of the United States Government. Neither the United States Government nor any agency thereof, nor any of their employees, makes any warranty, express or implied, or assumes any legal liability or responsibility for the accuracy, completeness, or usefulness of any information, apparatus, product, or process disclosed, or represents that its use would not infringe privately owned rights. Reference herein to any specific commercial product, process, or service by trade name, trademark, manufacturer, or otherwise does not necessarily constitute or imply its endorsement, recommendation, or favoring by the United States Government or any agency thereof. The views and opinions of authors expressed herein do not necessarily state or reflect those of the United States Government or any agency thereof.

DISTRIBUTION OF THIS DOCUMENT IS UNLIMITED

DISCLAIMER

This report was prepared as an account of work sponsored by an agency of the United States Government. Neither the United States Government nor any agency thereof, nor any of their employees, makes any warranty, express or implied, or assumes any legal liability or responsibility for the accuracy, completeness, or usefulness of any information, apparatus, product, or process disclosed, or represents that its use would not infringe privately owned rights. Reference herein to any specific commercial product, process, or service by trade name, trademark, manufacturer, or otherwise does not necessarily constitute or imply its endorsement, recommendation, or favoring by the United States Government or any agency thereof. The views and opinions of authors expressed herein do not necessarily state or reflect those of the United States Government or any agency thereof.

DISCLAIMER

Portions of this document may be illegible in electronic image products. Images are produced from the best available original document.

Abstract

Silicon and helium elastic recoil detection (ERD) have been used to obtain concentration versus depth profiles of hydrogen (^1H) and deuterium (^2H) in polymers. Using helium ERD, a depth resolution of 100nm was achieved in polystyrene, whereas 30nm was achieved using silicon ERD. Polymers are in general susceptible to radiation damage and precautions are necessary in order to minimize this. These precautions are addressed. When helium ERD is used to obtain the yield versus energy profile, the conversion of this profile to one of concentration versus depth is relatively straightforward since the scattering cross sections for collisions between helium and ^1H or ^2H nuclei are independent of energy over typical incident energy ranges (2.3 -3.0 MeV) used in these studies. With the use of silicon ions, corrections for the energy dependence of the scattering cross section must also be made. A comparison of helium ERD measurements of diffusion in polymer systems is made with those obtained using other techniques. The agreement is excellent.

Introduction

Whereas backscattering spectrometry [1] is well suited for the elemental analysis of medium to heavy elements, elastic recoil detection (ERD) [2-7], first introduced over a decade ago, is ideally suited for the analysis of light elements, such as hydrogen and its isotopes, where the mass selection rules prohibit the use of backscattering spectrometry. ERD has very good depth resolution, it has high sensitivity and is relatively simple. Its main advantage over nuclear reaction analysis [8] is that it can profile multiple elements simultaneously; nuclear reaction analysis, though its use is not restricted to the analysis of elements of any mass range, determines the energy and yield of a specific nuclear reaction. ERD has recently been used in a number of areas of scientific and technological interest that concern polymers. It has been used to investigate the fundamental aspects of the dynamics of polymeric molecules [5, 9-17]. The segregation of molecules near interfaces [18] and surfaces [19] in polymer alloy melts and the understanding of the thermodynamics of polymer alloy melts [20-22] have also been studied using ERD. ERD has recently been used for microelectronics applications involving polymers [23]. The purpose of this paper is to address the use of light and heavy ion ERD for the profiling of hydrogen and deuterium primarily in polymeric materials. A brief discussion of an application of the use of ERD to study the dynamics in polymeric systems is also presented. The results are discussed in light of those obtained using other techniques [6].

Fundamantals of ERD

A schematic of the ERD experiment is shown in Figure 1. Here a monoenergetic beam of ions of energy E_0 (MeV) impinges on a target at an angle θ_1 with

respect to the target normal. Some of these incident ions undergo kinematic collisions with the target nuclei and this results in the recoil of some of these nuclei at angles θ. A nucleus that recoils from the surface has an energy E_2 which is related to E_0 by

$$E_2 = KE_0 \tag{1}$$

where

$$K = \frac{4M_rM_p}{(M_p + M_r)^2}\cos^2\theta$$

is the kinematic factor for elastic scattering. M_p is the mass of a projectile and M_r is the mass of a recoil. It is clear that through knowledge of E_0, M_p M_r and θ and measurement of E_2that ERD can be used to identify light elements at the surface of solids. A particle that recoils from a depth x beneath the surface leaves the sample with energy E_3

$$E_3 = KE_0 - [S]x \tag{2}$$

[S] is defined in terms of the stopping powers S_1 of the projectile as it traverses the sample and S_2 of the recoiling nucleus as it travels out of the sample. If the target is sufficiently thin that S_1 and S_2 can be assumed to be approximately constant, independent of energy, then

$$[S] = \frac{KS_1}{\cos\theta_1} + \frac{S_2}{\cos\theta_2} \tag{3}$$

The energy with which a particle is detected is given by

$$E_d = KE_0 - [S]x - \Delta E_{foil} \quad (4)$$

where ΔE_{foil} represents the energy that a recoil loses upon traversing a range foil placed in front of a silicon surface barrier detector in order to prevent any of the forward scattered projectiles from reaching the detector. From this measurement a spectrum of particle yield (i.e. the number of particles detected with energy E_d whose energy lies between $E_d+\delta E_d/2$ and $E_d-\delta E_d/2$, where δE_d is the width of an energy channel in the multichannel analyser) versus E_d is obtained. Based on Eq. 4, the relation between the depth scale, x, and the detected particle energy, E_d, is unambigiously determined. The concentration of nuclei, N(x) at a given depth x may be expressed in terms of the scattering cross-section $\sigma(E_1,\theta)$, and the recoil yield, $Y_r(E_d)$ [3],

$$Y_r(E_d) = \frac{\Phi_p N(x)\, \sigma(E_1,\theta)\, \Omega\, \delta E_d}{\cos\theta_1 \frac{dE_d}{dx}} \quad (5)$$

In the above equation Φ_p is the flux of incident particles, Ω is the solid angle subtended by the detector and E_1 is the energy of a projectile just before a collision. The parameter dE_d/dx is the effective stopping cross section of the recoils in the range foil and is given by [3]

$$\frac{dE_d}{dx} = R[S] \quad (6)$$

Here $R=S(E_d)/S(E_3)$, which is the ratio of the stopping powers of the recoil at the surfaces of the range foil at energies E_3 and E_d. In some cases the

scattering process may be described by the Rutherford formula which, if defined in terms of the laboratory coordinates, is given by [1]

$$\sigma(E_1,\theta) = \left[\frac{Z_p Z_r e^2 (M_p+M_r)}{2M_r E_1} \right]^2 \frac{1}{(\cos\theta)^3} \qquad (7)$$

Z_p and Z_r are the atomic numbers of the projectile and recoils, respectively, and e is the charge of an electron. In situations where the scattering cross section is not well known, such as the recoil of protons (^1H) and of deuterons (^2H) by helium ions, an alternative procedure may be used. This is addressed later.

In practice, the targets are thick and S_1 and S_2 are therefore not constant. Under these conditions the following procedure [4] is used to determine the depth scale. The sample is divided into n sublayers (Figure 2) each sufficiently thin that S_1 and S_2 are essentially constant within each layer. The energy of a projectile at the n'th interface is given by the recursion relation

$$E_0^{(n)} = E_0^{(n-1)} - xS_p^{(n)}(E_0^{(n-1)}) \qquad (8)$$

where the index, n, denotes the layer. $S_p^{(n)}(E_0^{(n-1)})$ is the stopping power of the projectile traveling through the n^{th} layer; $E_0^{(n-1)}$ is the energy of the projectile at the interface between the (n-1)'th and n'th layer. Note here that $E_0 = E_0^{(0)}$. The concentration, $N_r^{(n)}(x^{(n)})$, of recoils at the n'th interface is expressed in terms of the recoil yield, $Y_r^{(n)}(E_d)$, at the n'th interface [4]

$$Y_r^{(n)}(E_d) = \frac{\Phi_p N_r^{(n)}(x^{(n)})\,\sigma(E_0^{(n)}, \theta)\,\Omega\,\delta E_d}{\cos\theta_1 \frac{dE_d}{dx^{(n)}}} \tag{9}$$

Φ_p and Ω are as previously defined and the scattering cross section is defined at energy $E_0^{(n)}$ at the n'th interface. The effective stopping power of particles that recoil from the n'th interface now have a much more complicated form [4]

$$\frac{dE_d}{dx^{(n)}} = \Pi_n [S]_{p,r}^{(n)} \tag{10}$$

where

$$\Pi_n = \frac{S_r^{(n)}(E_3^{(n)})}{S_r^{(n)}(E_2)} \cdot \frac{S_r^{(n-1)}(E_3^{(n-1)})}{S_r^{(n-1)}(E_3^{(n)})} \cdots \frac{S_r^{(0)}(E_d)}{S_r^{(0)}(E_3^{(1)})}$$

Each term in this product represents the ratio of the stopping powers of the recoil energies at the interfaces of a given layer. The stopping power $[S]_{p,r}^{(n)}$ is defined [4] in terms of $S_p^{(n)}$ the stopping power of the projectile in the n'th layer, and of $S_r^{(n)}$, the stopping powers of a recoil in the n'th layer,

$$[S]_{p,r}^{(n)} = K\frac{S_p^{(n)}(E_0^{(n)})}{\cos\theta_1} + \frac{S_r^{(n)}(E_2^{(n)})}{\cos\theta_1} \tag{11}$$

$E_1 = E_0^{(n)}$ is the energy of the projectile at the n'th interface just before a collision and $E_2^{(n)}$ is the energy of the recoil instanteneously after a collision. These equations provide the general framework within which ERD data may be analyzed. In summary, at each interface one calculates $E_3^{(n)}$, $E_1^{(n)}$, $E_2^{(n)}$,

$[S]_{p,r}^{(n)}$, dE_d/dx and $\sigma(E_1,\theta)$ (the Rutherford scattering formula is not always applicable).This information will enable the determination of the concentration versus depth scale from the recoil yield versus detected energy scale.

In conducting these experiments one has control over a number of parameters such as the incident beam energy as well as the incident and exit angles, θ_1 and θ_2 and the thickness of the range foil. The choice of these parameters will influence the sensitivity, the probing depth and the depth resolution of this technique. The depth resolution, (δx), of the experiment can be expressed in terms of the effective stopping powers dE_d/dx [3]

$$(\delta x) = \frac{\delta E_d}{dE_d/dx} \qquad (12)$$

In the ERD experiment, the most important contribution to the depth resolution is the energy straggling of the recoils in the range foil and the foil thickness nonuniformities. Another very important factor is the detector resolution. Other factors that contribute to the depth resolution, though considerably less important, are the sample surface roughness, the angular spread of the beam and the energy straggling of the projectile and the recoils in the target (target is usually considerably thinner than the range foil). The sensitivity of the experiment is primarily determined by the scattering cross section. A detailed discussion of the factors that influence the sensitivity, probing depth and the depth resolution may be found elsewhere [4,24,25].

Analysis of ^1H and ^2H in Polymers Using Light (Helium) Ions.

Consider the following example where the deuterium, ^2H, concentration is determined in a thick sample composed of a uniform mixture of polystyrene, PS, (hydrogen, ^1H to C ratio is 1:1) and deuteriated polystyrene, d-PS, (^2H:C=1:1). The sample has approximately 60% d-PS. The following analysis parameters were used: $\theta_1=\theta_2=75^0(\theta=30^0)$, E_0=2.8MeV M_p=4 (Helium); the range foil is mylar and it is of thickness 12μm. In addition a collimating slit was placed in front of a silicon surface barrier detector at a distance r= 5.08 cm; its height was h=1.69 cm and its width was w=0.16 cm. The spectrum of the recoil yield, $Y_r(E_d)$, versus energy, E_d, for the ^2H is shown in Figure 3. This spectrum was obtained from the yield versus channel number, CN, profile as follows. The channel number, CN_0, of the front surface of the profile is first located. The kinematic factor for the collision is then calculated followed by a calculation of the energy that the recoil loses upon traversing the mylar foil using the stopping powers that are discussed in references 26 and 27. The energy loss calculation is performed by dividing the foil into 10 layers, each of equal thickness. The incident and recoil energies are calculated at each interface. When E_d is determined one now has the energy versus channel number E_d/CN scale, hence the profile in Figure 3. The profile of $Y_r(E_d)$ versus x can now be determined in a straightforward manner. The sample is divided into a series of 1000Å layers. At each interface the following parameters are determined: $E_0^{(n)}$, $E_3^{(n)}$, $[S]_{p,r}^{(n)}$, E_d, dE_d/dx and x. The $Y_r(E_d)$ versus x scale is consequently determined. The upper scale in Figure 4 shows the depth scale, x.

The determination of the concentration versus x scale is a separate issue and varies depending on the accelerating projectile and the target ions that are recoiled from the sample. For the present situation, helium ions recoiling ^1H and ^2H, this is straightforward. The scattering cross section for $\theta=30^0$ is

independent of energy over incident beam energy ranges of 2.2 to 3.2 MeV for helium [24]. Therefore the correction that should be made is the dependence of the yield on the effective stopping powers (cf. Eqn. 9). The yield is therefore multiplied by a factor $[dE_d/dx]/ [dE_d/dx)_{surface}]$. The circles in Figure 4 depict what happens to the data when this correction is made. Clearly, the concentration of ^2H, hence d-PS, is uniform in the sample. In many situations when other projectiles are used this correction, which is always necessary, is insufficient. For example, for silicon ions the scattering cross section is Rutherford ($\sigma \sim E^{-2}$). Therefore, in addition to accounting for the dependence of the yield on the effective stopping powers, as discussed above, the yield is mulitplied by the factor $E_d/E_d^2)_{surface}$ in order to account for the energy dependence of the scattering cross section. The volume fraction, or concentration, can now be obtained by dividing the spectrum by a constant factor. This constant factor is determined by using a standard of known composition. Figure 5 shows the profile of the standard composed only of ^2H and C at a 1:1 ratio. The filled symbols represent the uncorrected data and the + symbols represent the data corrected for the effective stopping power dependence of the yield. The volume fraction shown in Figure 4 was obtained by dividing the yield of the profile of the PS/d-PS mixture by that of the standard.

As a final example we may briefly discuss the analysis of ^1H in a 5000Å film composed of a mixture of d-PS and PS where the quantity of PS is 80% using 2.8MeV helium ERD. The analysis proceeds as discussed above; only corrections that account for the dE_d/dx dependence of Y_r are made. A pure PS standard, composed of only ^1H and C at a 1: 1 ratio, was used in order to obtain the volume fraction. Figure 6 shows the profiles. The + symbols represent the uncorrected data and the triangles represent the corrected data.

Use of Heavy ions for the Analysis of ^{2}H and ^{1}H

The use of heavy ions for the analysis of polymers offer a number of advantages over the use of light ions like helium. For example, the depth resolution of 0.7 MeV/amu helium ions in PS is 1000Å and for 0.7 MeV/amu silicon ions in PS it is 300Å. This is due to the much larger stopping powers of the Si ions in the material. The scattering cross sections are higher when Si ions are used which implies that Si ERD has greater sensitivity. The analysis range using silicon is also increased from 7000Å to 9200Å. The analysis range is limited by the energy at which the ^{2}H profile overlaps the front surface of the ^{1}H profile located at lower energies. Table 1 shows the improvement in depth resolution and analysis range with the use different ions. These advantages are, however, offset by radiation damage effects, addressed below.

Table 1

Ion	δx(FWHM), Å	Analysis range, Å
He	1000	7000
C	630	9400
Si	400	9200

Radiation effects

In general one will always encounter radiation damage effects when irradiating polymers with ion beams. The important question that should be asked is whether the density, and hence the depth scale, of the polymer is being altered during the analysis. Secondly is hydrogen or deuterium being

released during the analysis? In many practical situations one uses fluences ~10^{13}- 10^{14} ions/cm^2. The loss of ^{1}H and ^{2}H using He ERD is insignificant. When silicon ions of the same energy/amu are used the radiation damage is considerable. One loses up to 60% of ^{2}H for doses of $1.5x10^{13}$ ions/cm^2. The ^{2}H loss, however, is uniform along the ion "track". The same is true of the ^{1}H loss. A more serious problem, however, is the release of carbon during the process since the density of the polymer, hence the depth scale, is consequently altered. The carbon loss can be significant in some cases. This effect is insignificant in the case where helium ions are used. The large energy loss rates (large stopping powers) of the Si ions in the material is, evidently, primarily responsible for the increased damage to the material. Table 2 shows a comparision of the deuterium release that results when different ions of the same energy/amu, at comparable fluences, are used.

Table 2

Ion	F(10^{13}), #/cm^2	Fractional loss of ^{2}H
He	3.2	.002
C	5.6	0.2
Si	1.5	0.6

There are situations in which it the use of helium ions can be very distructive to polymers. For example, let us compare the damage that helium does to polystyrene versus polymethylmethacrylate (PMMA), an electron beam resist. Figure 7 shows the ^{1}H loss upon 3.0MeV helium ion irradiation of a 5000Å film of PMMA on a silicon substrate. The circles represent data that was obtained

after a total fluence of $1.2x10^{14}$ ions/cm^2; the + symbols represent data obtained after $2.5x10^{14}$ ions/cm^2 and the triangles after $5.0x10^{14}$ ions/cm^2. Approximately 20% of the ^1H is lost during the analysis. In comparison, these effects in polystyrene are insignificant. This example illustrates the difference between the damage done to one polymer that is known to be extremely susceptible to radiation damage (PMMA) and one the is comparatively radiation resistant (as far as polymers are concerned).

In performing the analysis much of the radiation damage can be minimized by using low beam currents $<5x10^{11}$ ions/cm^{2}sec. In some cases it may be helpful to perform experiments at low temperatures and to minimize the irradiation fluence required for the analysis.

Application of ERD to the Study of Polymer-Polymer Diffusion

As a separate example we may consider an application of ERD to the study of polymer-polymer diffusion. The results we obtain are compared with those obtained using other techniques. This example demonstrates the utility of ERD and, indeed, instills confidence in the use of ERD to study polymers.

The following is a short review of diffusion in polymer-polymer systems. For further details the interested reader is encouraged to consult reference 30. Consider a polymer chain composed of N units where each unit has a molecular weight of M_0 grams/mol, then the total molecular weight of the chain is $M=M_0N$. In a polymer melt, this chain, provided it is sufficiently long, is highly entangled with other chains. It is compelled to diffuse by snake-like motions since its lateral excursions are restricted by the neighboring chains. The motion of the N-chain is therefore imagined to occur within the confines of a virtual "tube" formed by the locus of its intersections with its neighbors. If the surrounding chains are sufficiently long it may be shown that the diffusion coefficient of the N-chain is given by $D^*= D_0M^{-2}$[30]. The prefactor,

D_0, depends on the molecular structure of the polymer system.

Below we show how ERD has been used to understand this process. A diffusion couple is set up where a thin layer of d-PS (20nm) was placed in contact with thick layer (~4 μm) of PS. The molecular weight, $M=5.2\times10^5$, of the d-PS was chosen such that it was considerably less than the molecular weight, P, of the PS host ($P=2.0\times10^7 << M_H$). The diffusion process was allowed to commence at 171°C for 2.9 hours. During this period the d-PS composition became very dilute in the PS host. Figure 8a shows the 3.0 MeV helium yield versus E_d profile of the system after it was allowed to diffuse. The ^2H profile is seen at high energies and the ^1H profile at lower energies. Shown in figure 8b is the profile of volume fraction, $\Phi(x)$, versus depth of the d-PS into the PS host. The diffusion coefficient, D*, of the d-PS chains into the PS host was obtained using the following equation [28]:

$$\Phi(x) = \frac{1}{2}\left\{ \mathrm{erf}\left[\frac{(H+x)}{(4D^*t)^{1/2}}\right] + \mathrm{erf}\left[\frac{(H-x)}{(4D^*t)^{1/2}}\right]\right\} \qquad (13)$$

The line drawn through the data is a convolution of this equation with the instrumental resolution function which is assumed to be Gaussian with a FWHM of 100nm. The value of D* was adjusted to gave the best fit to the data. In the above equation, H is the initial thickness of the d-PS layer. The diffusion coefficient is $D^*=2.8\times10^{-14}$ cm^2sec^{-1}. Shown in Figure 9 are plots of the diffusion coefficients in the polystyrene/polystyrene system determined using different techniques. The + symbols represent the diffusion coefficients obtained from our ERD measurements of d-PS into PS. The squares represent the diffusion coefficient obtained by studying the diffusion of PS into d-PS [6] in separate ERD studies performed at Cornell University. The triangles represent data for the diffusion of d-PS into PS [7], performed in the same place. The circles represent data obtained using a holographic grating

technique [30]. The agreement between all sets of data is excellent. These data mentioned here are also in excellent agreement with RBS data, not shown here, obtained using a marker displacement technique [6, 31].

Finally we may compare helium and silicon ERD measurements of the diffusion coefficients of a d-PS chain of moleculer weight M diffusing into PS hosts of varying molecular weights, P. From Figure 10 it is clear the D*'s obtained using Si ions are a factor of 2 smaller than those obtained using helium ions. This difference, as we have previously shown, is due to the fact that the Si ions alter the depth scale of the PS host.

In conclusion ERD is an powerful technique with which to analyze polymers. Its main advantages are that is can profile multiple elements simultaneously, it has good depth resolution, high sensitivity and is relatively simple to use. It has been applied to a variety of problems of scientific and technological interest. There are some situations in which the radiation damage is excessive but damage may be minimized using low beam currents and in some cases performing experiments at low temperatures. One should also minimize the fluences needed to determine profiles. For some systems, such as He ion irradiation of polystyrene, the radiation damage is minimal as demonstrated above. In other cases it may be significant. Therefore, it is important to exercise caution when choosing analysing particle beams and the polymers that they are intended to analyse.

*This work, performed at Sandia National Laboratories, was supported by the US Department of Energy under contract number DE-AC04-76DP00789.

FIGURE CAPTIONS

Figure 1. Schematic of the ERD experiment.

Figure 2. Sample divided into n sublayers, each of thickness $x^{(n)}$.

Figure 3. 2.8 MeV helium ERD Recoil yield versus detected energy profile of ^2H in a ^1H-PS/^2H-PS mixture.

Figure 4. The depth and the ^2H (^2H-PS) volume fraction scale of the profile in figure 3 are shown. The circles represent the data where only the dE_d/dx correction to the yield is made.

Figure 5. 2.8 MeV profile of a pure ^2H-PS standard where the ^2H:C ratio is 1:1 (sample contains 2% ^1H). The + symbols represent the corrected data (dE_d/dx correction only) and the filled circles represent the raw yield versus energy data. This profile was used to determine the volume fraction scale found in figure 4.

Figure 6. This is a 2.8 MeV ^1H profile of a ^1H-PS/^2HPS mixture. The triangles represent the corrected data (dE_d/dx corrections only) and the + symbols represent the raw yield versus Ed data. The depth and volume fraction scales are also shown.

Figure 7. Effect of 3.0 MeV helium ion irradiation on the ^1H concentration and depth scale on polymethylmethacrylate (PMMA).

Figure 8. a) 3.0 MeV helium Y_r vs. E_d profile of a thin layer (~20nm) of ^2H-PS after it diffused into a ^1H-PS host. The ^2H profiles is seen at higher

energies and the ^{1}H at lower energies.

b) Volume fraction versus depth profile of 2H-PS in 1H-PS. The solid line is a fit to the experimental data.

Figure 9. Comparison of the diffusion coefficients of polystyrene chains of molecular weight M which diffused into high molecular weight polystyrene hosts. The circles represent data obtained using a holographic grating technique (ref. 29). The squares and triangles represent 3.0 MeV ERD data obtained at Cornell University and the + symbors represent data obtained in this study.

Figure 10. Comparison of helium versus silicon ERD studies of diffusion in polystyrene.

REFERENCES AND NOTES

1. W.K.Chu, J.W. Mayer and M.A. Nicolet, Backscattering Spectrometry, (Academic Press: New York, 1978).
2. J. L'Eucyler, C. Brassard, C. Cardinal, J. Chabbal, L. Deschenes, J.P Labrie, B. Terrault, J.G. Martel and St. -Jacues, J. Appl. Phys. 47, 381 (1976).
3. B.L. Doyle and P.S. Peercy, Appl. Phys. Lett. 34, 811 (1979), B.L. Doyle and P.S. Peercy, Internal Sandia National Laboratories Report, SAND79-02106 (1979).
4. B.L. Doyle and D.K. Brice, Nuclear Instruments and Methods in Physics Research, B35, 301 (1988)
5. P.F. Geen and B.L. Doyle, Characterization Techniques for Thin Polymer Films, edited by Ho Ming Tong (Wiley, New York 1989, to be published)
6. P.F. Green, P.J. Mills and E.J. Kramer, Polymer, 27, 1063, (1986).
7. P.J. Mills,P.F. Green, C.J. Palmstrom, J.W. Mayer and E.J. Kramer, Appl. Phys. lett. 45, 958 (1984)
8. G. Amsel, J.P. Nadai, E. d'Artemare, D. David, E. Girard and J. Moulin, Nuclear Instruments and Methods, 92, 481 (1971); R.A. Langley, S.T. Picraux and F.L. Vook, J. Nuclear Materials, 53, 257 (1974); C. Cardinal, C. Brassard, J. Chabbal, L. Deschenes, J.P Labrie, J. L'Eucyler, M.Lernoux, Appl. Phys. Lett., 26, 543 (1975)
9. P.F. Green, P.J. Mills, C.J. Palmstrom, J.W. Mayer and E.J. Kramer, Phys. Rev. Lett. 53, 2145, (1984).
10. P.F. Green and E.J. Kramer, Macromolecules, 19, 1108, (1986).
11. S.F. Tead and E.J. Kramer, Macromolecules, 21, 1513 (1988).
12. K.R. Schull, E.J. Kramer, G. Hadziioannou, M. Antonietti and H. Sillescu, Macromolecules, 21, 2578 (1988).
13. P.F. Green, T.P. Russell, M. Granville and R.Jerome, Macromolecules, 21, 3266, (1988).
14. P.F. Green, T.P. Russell, M. Granville and R.Jerome, Macromolecules, 22, 908 (1989).
15. P.F. Green, New Trends in The Physicasl and Physical Chemistry of Polymers, Editor S.Lee (to be published 1989)
16. P. F. Green and E.J. Kramer, J. Mat. Res.1, 202 (1986).
17. P.F. Green and B.L. Doyle, Nuclear Instruments and Methods in Physics Research,

B35, 64 (1986)

18. P.F. Green and T.P. Russell, Unpublished results
19. R.A.L. Jones, E.J. Kramer, M.H. Rafailovich, J. Sokolov and S.A. Schwarz, Phys .Rev. Lett. 62, 280 (1989).
20. P.F. Green and B.L. Doyle, Phys. Rev. Lett., 57, 2407, (1986); Macromolecules, 20, 2471, (1987).
21. R.J. Composto, J.W. Mayer, E.J. Kramer and D.M. White, Rhys. Rev. Lett. 57, 1312 (1986).
22. R.J. Composto, E.J. Kramer and D.M. White,Nature, 323, 1980 (1987).
23. S.F. Tead, W.E. Vanderline, A.L. Ruoff and E.J. Kramer, Appl. Phys. Lett 52, 101 (1988)
24. S. Nagata, S. Yamaguchi, Y. Fujino, Y. Hori, N. Sugiyama and K. Kamada, Nuclear Instruments and Methods in Physics Research B6, 533 (1985).
25. A. Turos and O. Meyer, Nuclear Instruments and Methods in Physics Research B4, 92, (1984).
26. J.F. Zeigler, The Stopping Powers and Ranges of Ions in Materials, Vol. 4: H.H. Anderson and J.F. Zeigler, ibid Vol. 3 (Pergamon Press, N.Y. (1977)).
27. D.K. Brice, Physical Review A, 6, 1791 (1972).
28. J. Crank, The Mathematics of Diffusion, 2nd Ed. (Oxford University press Oxford, U.K. 1975).
29. M. Antonietti, J. Coutandin and H. Sillescu, Macromol. Chem. Rapid Commun. 5, 525 (1984).
30. M. Doi ans S.F. Edwards, Theory of Polymer Dynamics (Oxford Univ. Press, Oxford U.K. 1988).
31. P. F. Green, C. J. Palmstrom, J. W. Mayer and E.J. Kramer, Macromolecules, 18, 501, (1985).

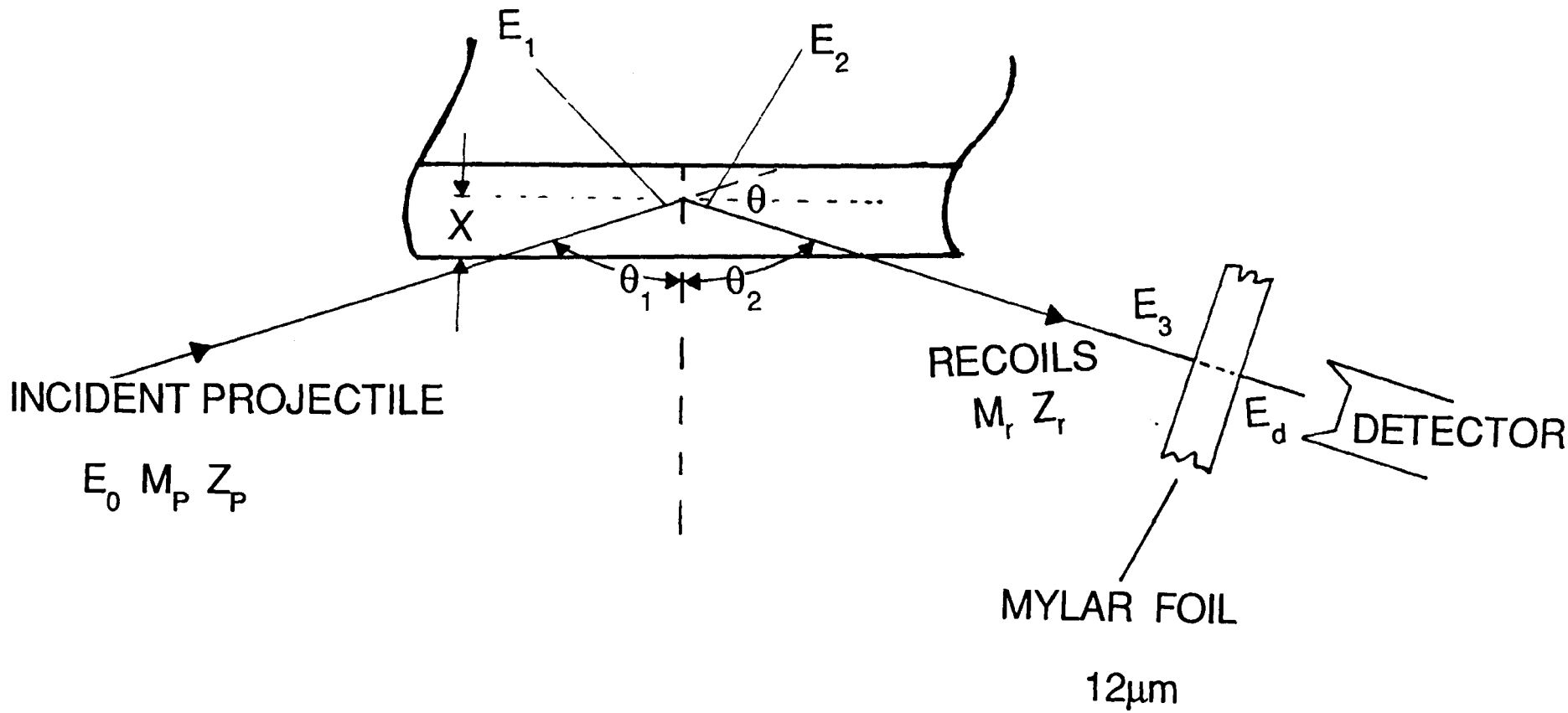
E1
E2
X
θ
θ1
θ2
INCIDENT PROJECTILE
E0 MP ZP
RECOILS
Mr Zr
E3
Ed
DETECTOR
MYLAR FOIL
12μm

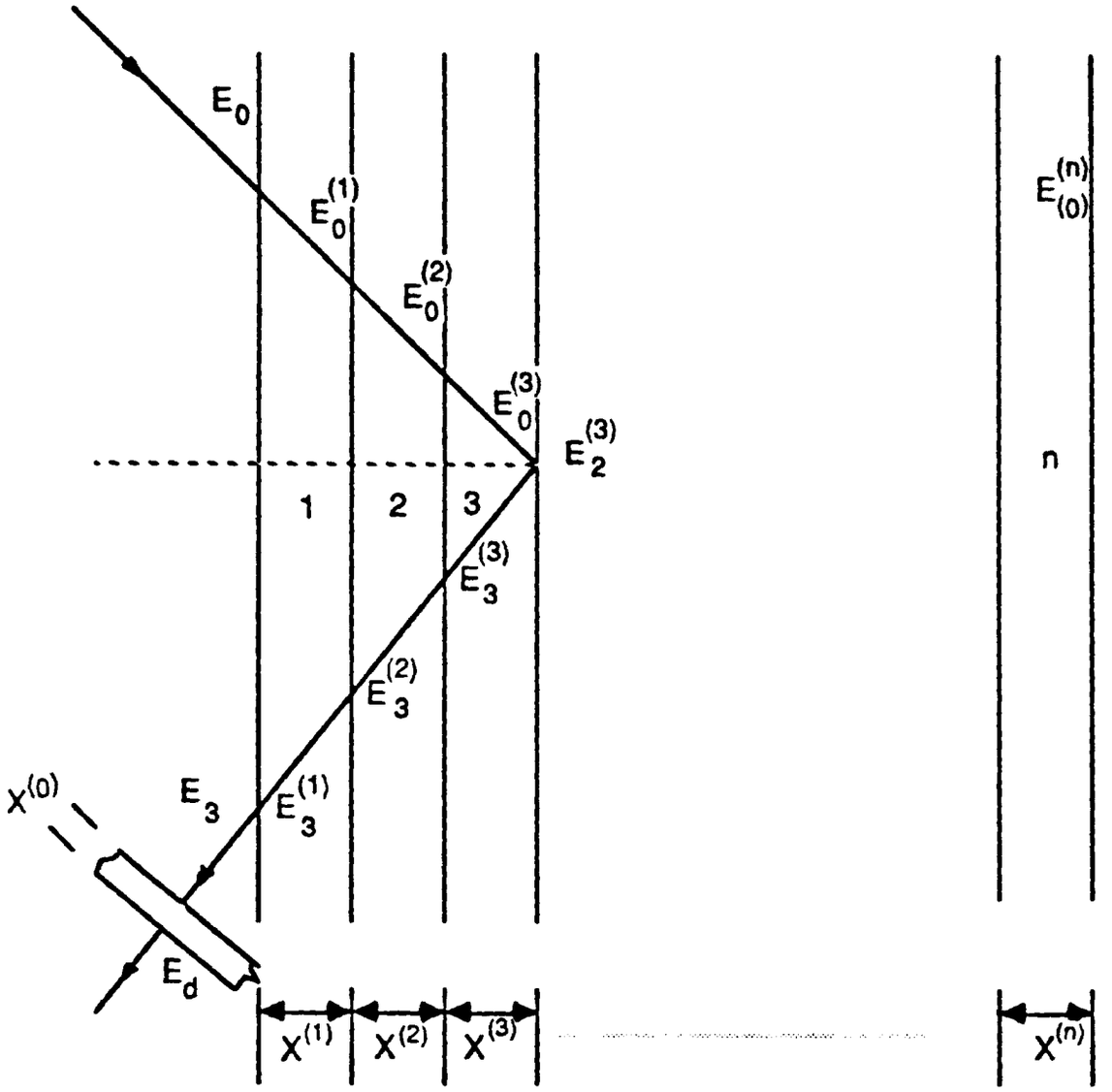

FIG. 2

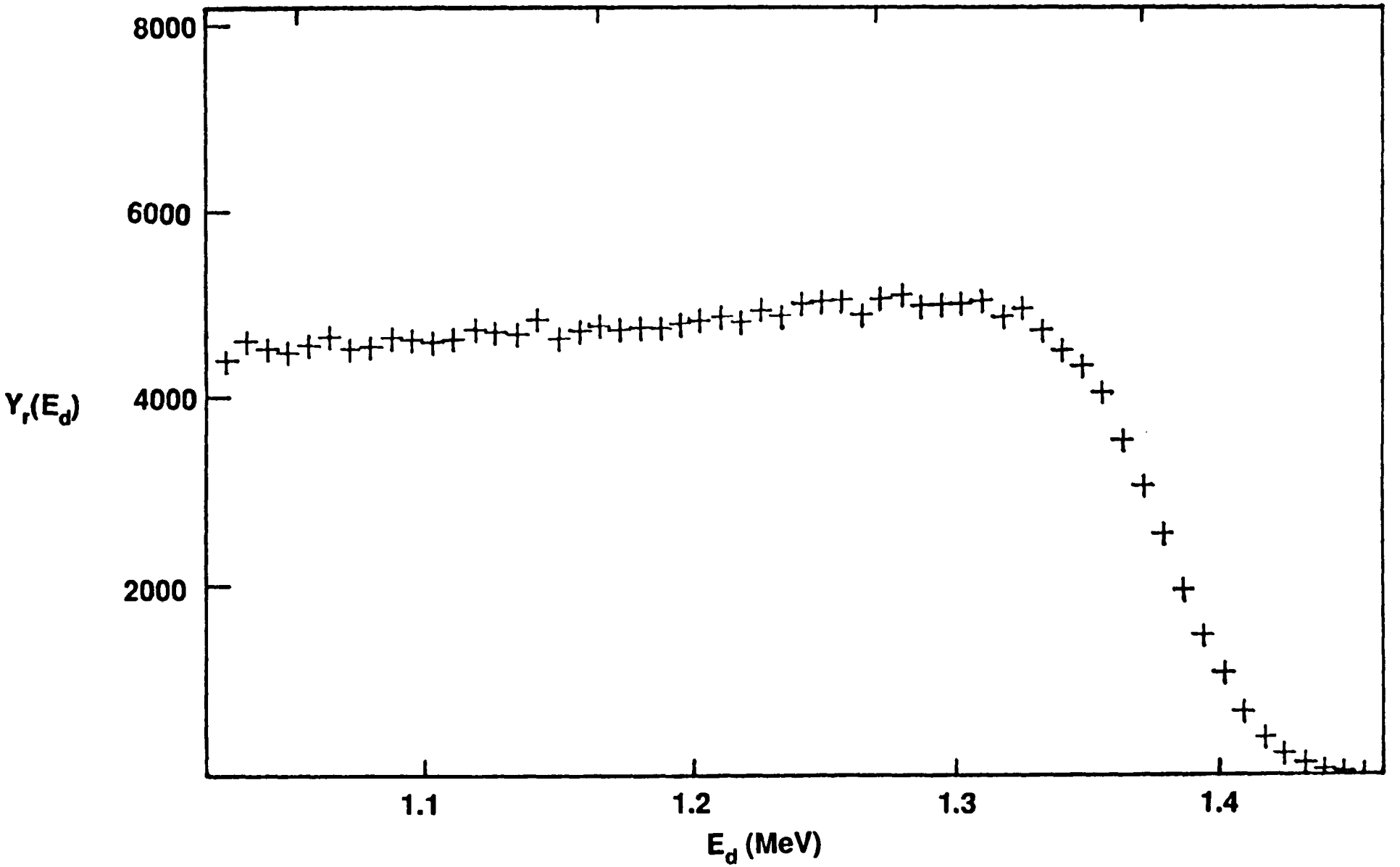

FIG. 3

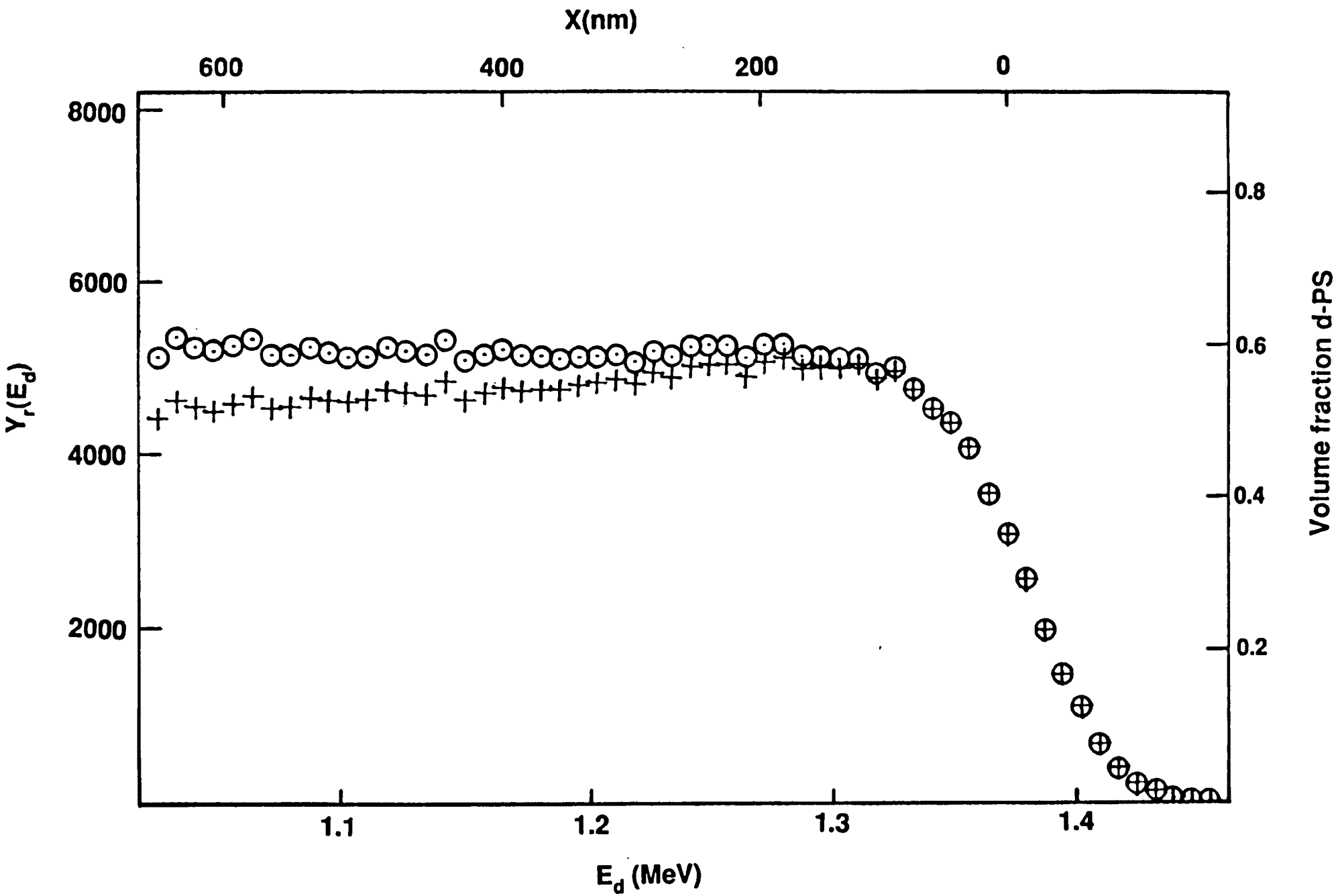
X(nm)
600
400
200
0
8000
6000
4000
2000
$Y_r(E_d)$
0.8
0.6
0.4
0.2
Volume fraction d-PS
1.1
1.2
1.3
1.4
E_d (MeV)

FIG 4

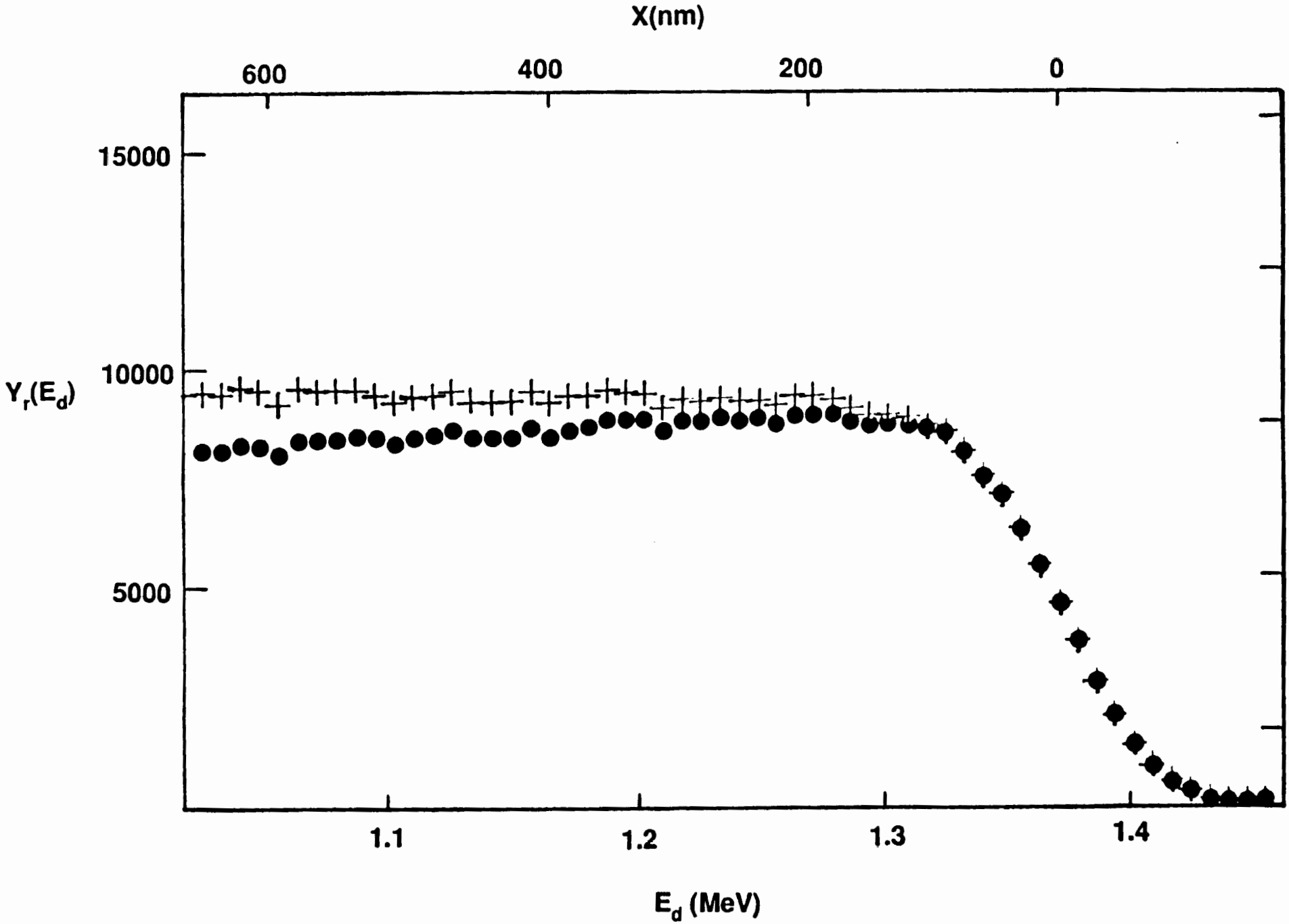

FIG. 5

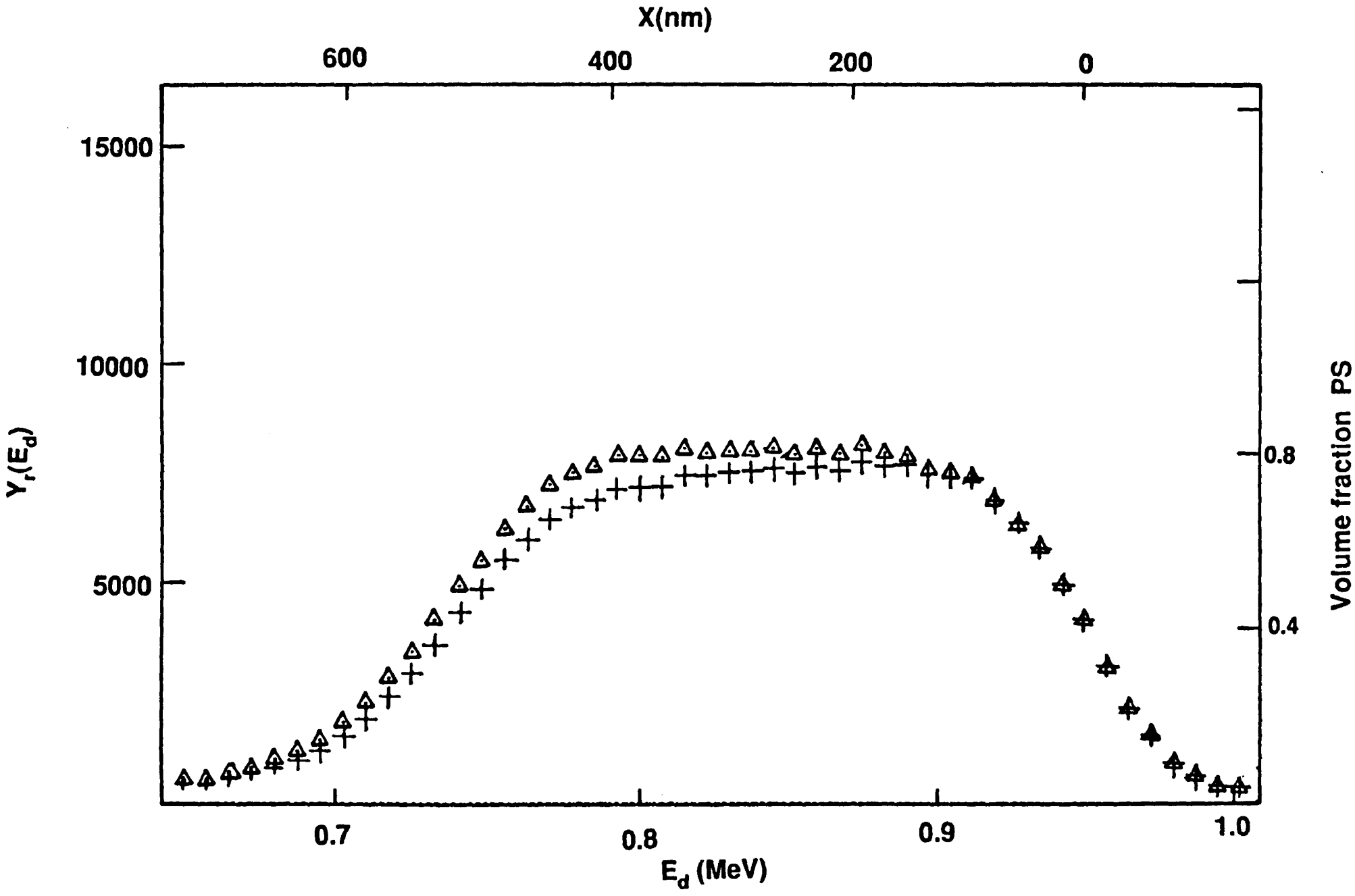
X(nm)
600
400
200
0
15000
10000
5000
$Y_r(E_d)$
0.8
0.4
Volume fraction PS
0.7
0.8
0.9
1.0
E_d (MeV)

FIG. 6

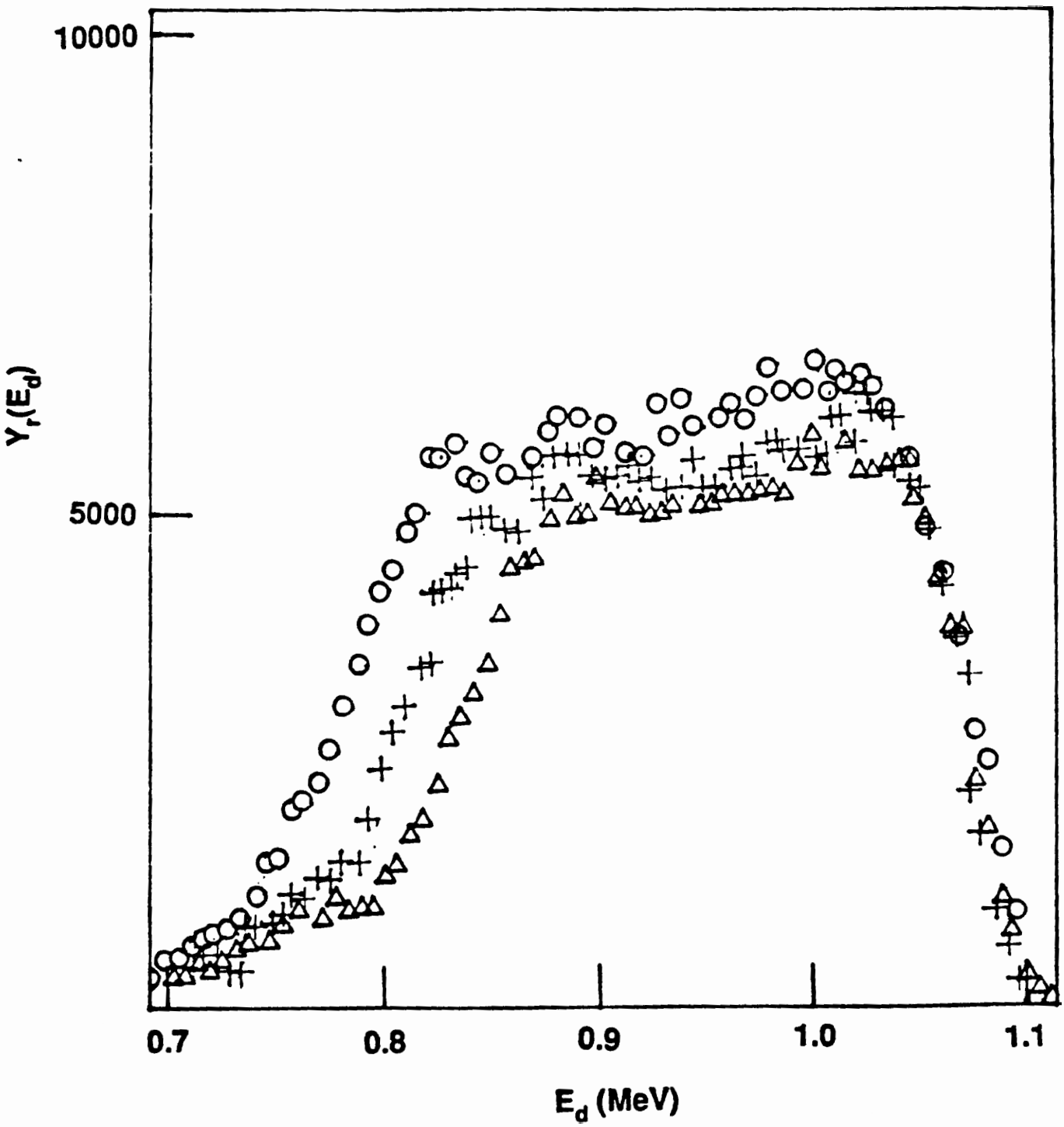
10000
5000
$Y_r(E_d)$
0.7
0.8
0.9
1.0
1.1
E_d (MeV)

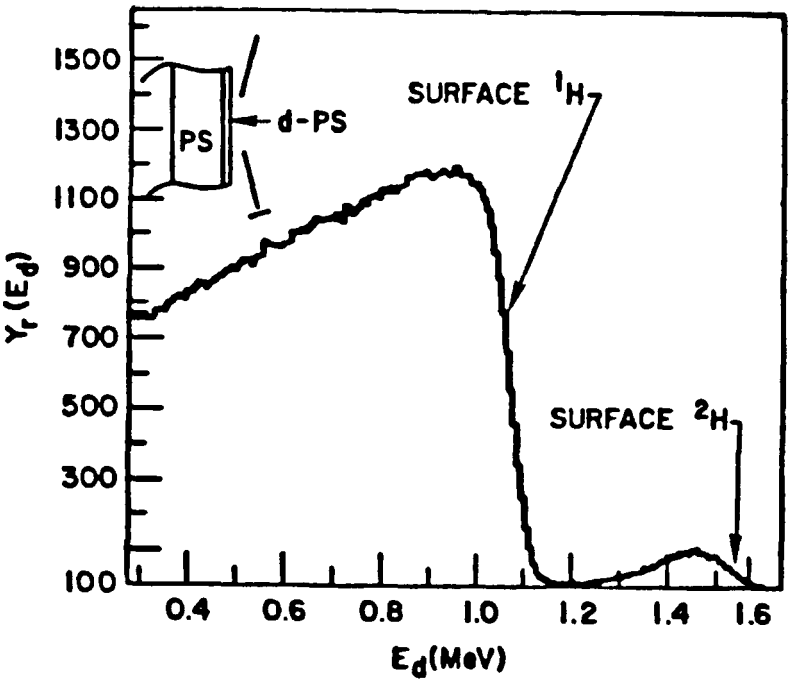
1500
1300
1100
900
700
500
300
100
PS
d-PS
SURFACE ^{1}H
SURFACE ^{2}H
$Y_r(E_d)$
0.4
0.6
0.8
1.0
1.2
1.4
1.6
E_d(MeV)

(a)

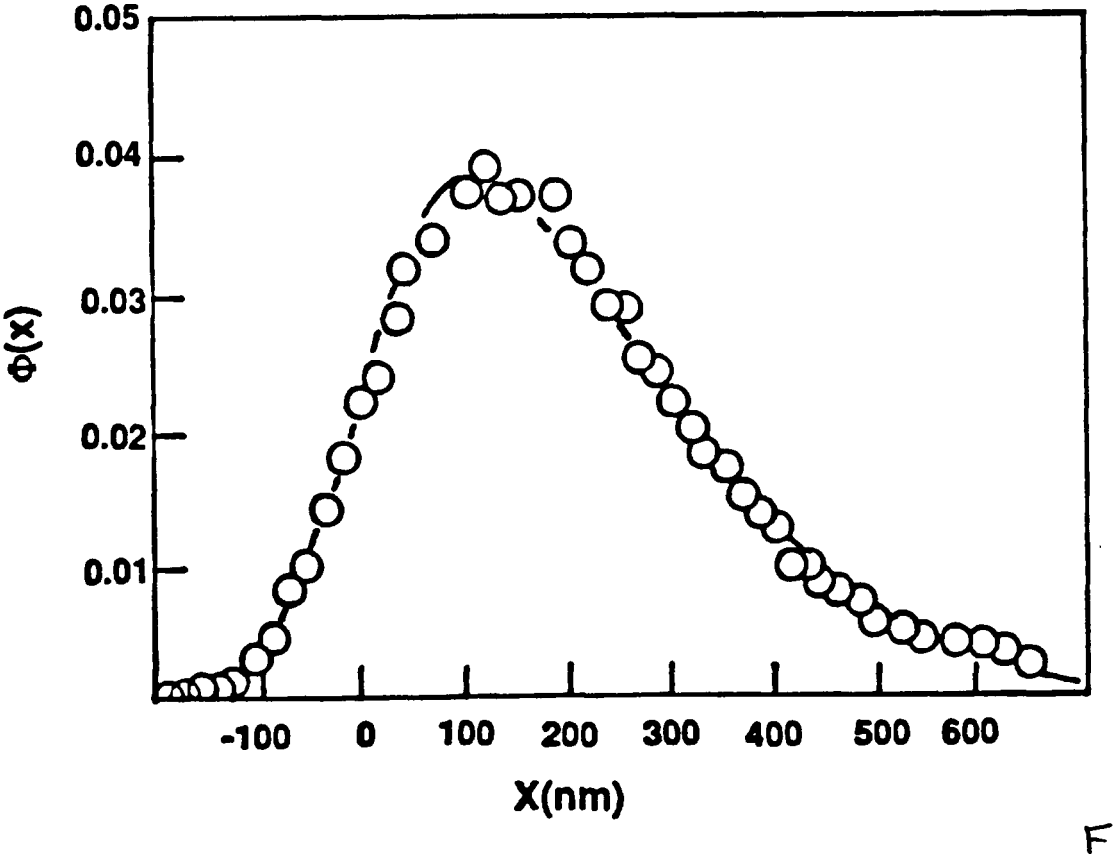
0.05
0.04
0.03
0.02
0.01
Φ(x)
-100
0
100
200
300
400
500
600
X(nm)

(b)

FIG.8

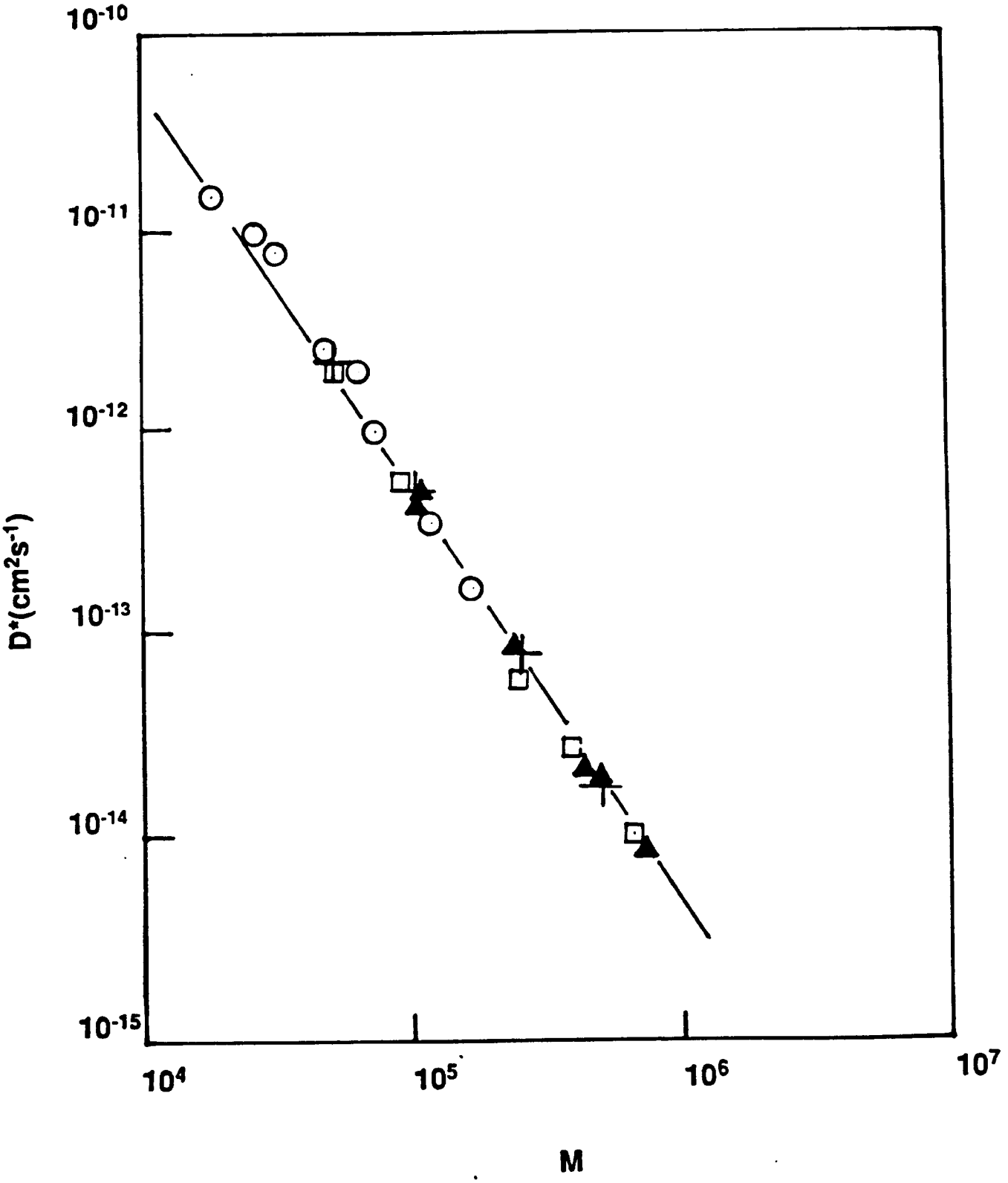

FIG. 9

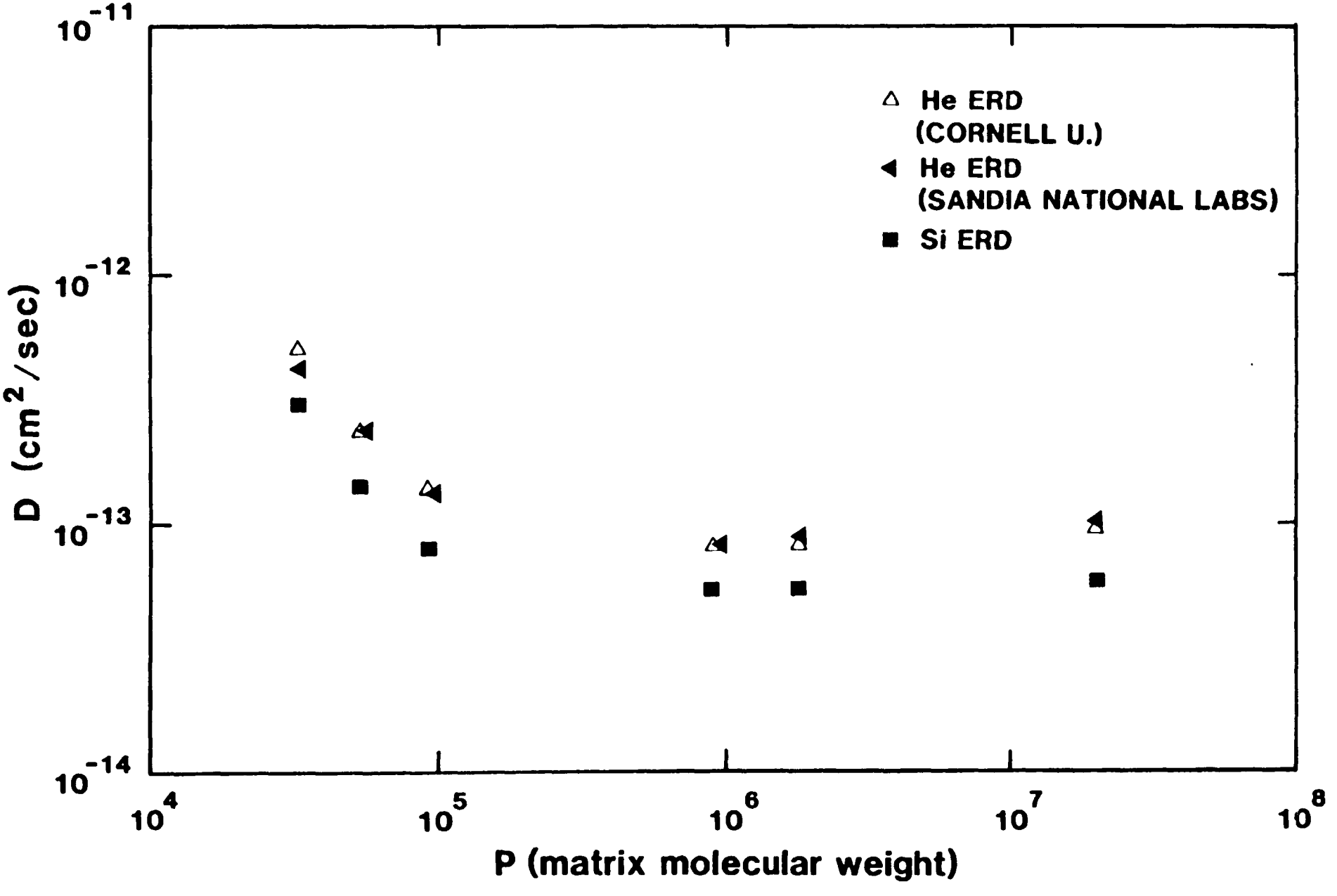
10^{-11}
10^{-12}
10^{-13}
10^{-14}
D (cm^2/sec)
10^4
10^5
10^6
10^7
10^8
P (matrix molecular weight)
△ He ERD (CORNELL U.)
◀ He ERD (SANDIA NATIONAL LABS)
■ Si ERD

FIG. 10